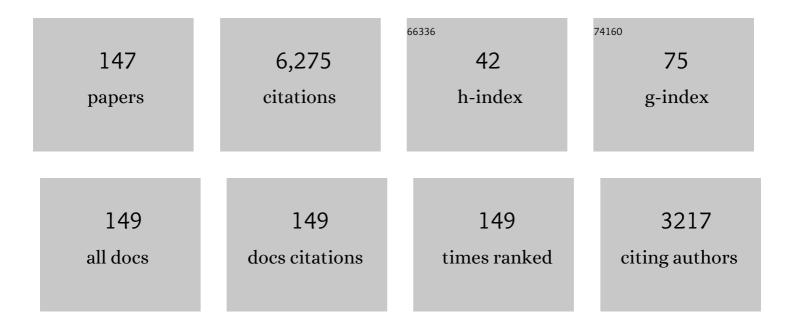
## Jayanta Das

List of Publications by Year in descending order

Source: https://exaly.com/author-pdf/1797017/publications.pdf Version: 2024-02-01



ΙΛΥΛΝΤΛ ΠΛΟ

#	Article	IF	CITATIONS
1	"Work-Hardenable―Ductile Bulk Metallic Glass. Physical Review Letters, 2005, 94, 205501.	7.8	857
2	Mechanical properties of bulk metallic glasses and composites. Journal of Materials Research, 2007, 22, 285-301.	2.6	386
3	Is the energy density a reliable parameter for materials synthesis by selective laser melting?. Materials Research Letters, 2017, 5, 386-390.	8.7	294
4	Deformation-induced martensitic transformation in Cu–Zr–(Al,Ti) bulk metallic glass composites. Scripta Materialia, 2009, 60, 431-434.	5.2	166
5	Heterogeneity of a Cu47.5Zr47.5Al5 bulk metallic glass. Applied Physics Letters, 2006, 88, 051911.	3.3	152
6	High-strength Ti-base ultrafine eutectic with enhanced ductility. Applied Physics Letters, 2005, 87, 161907.	3.3	151
7	Effect of aspect ratio on the compressive deformation and fracture behaviour of Zr-based bulk metallic glass. Philosophical Magazine Letters, 2005, 85, 513-521.	1.2	145
8	High strength Ti–Fe–Sn ultrafine composites with large plasticity. Scripta Materialia, 2007, 57, 101-104.	5.2	133
9	Improved plasticity of bulk metallic glasses upon cold rolling. Scripta Materialia, 2010, 62, 678-681.	5.2	128
10	High strength ductile Cu-base metallic glass. Intermetallics, 2006, 14, 876-881.	3.9	123
11	High-strength Zr-Nb-(Cu,Ni,Al) composites with enhanced plasticity. Applied Physics Letters, 2003, 82, 4690-4692.	3.3	108
12	Tunable (violet to green) emission by high-yield graphene quantum dots and exploiting its unique properties towards sun-light-driven photocatalysis and supercapacitor electrode materials. Materials Today Communications, 2017, 11, 76-86.	1.9	96
13	Fabrication and mechanical properties of Ni–Nb metallic glass particle-reinforced Al-based metal matrix composite. Scripta Materialia, 2006, 54, 1445-1450.	5.2	95
14	Microscopic deformation mechanism of a Ti66.1Nb13.9Ni4.8Cu8Sn7.2 nanostructure–dendrite composite. Acta Materialia, 2006, 54, 3701-3711.	7.9	93
15	Phase stability and its effect on the deformation behavior of Ti–Nb–Ta–In/Cr β alloys. Scripta Materialia, 2006, 54, 1943-1948.	5.2	93
16	Dynamic softening and indentation size effect in a Zr-based bulk glass-forming alloy. Scripta Materialia, 2007, 56, 605-608.	5.2	88
17	Wavy cleavage fracture of bulk metallic glass. Applied Physics Letters, 2006, 89, 251917.	3.3	83
18	Modeling deformation behavior of Cu–Zr–Al bulk metallic glass matrix composites. Applied Physics Letters, 2009, 95, .	3.3	77

#	Article	IF	CITATIONS
19	Plasticity induced by nanoparticle dispersions in bulk metallic glasses. Journal of Non-Crystalline Solids, 2007, 353, 327-331.	3.1	76
20	Phase formation and thermal stability in Cu–Zr–Ti(Al) metallic glasses. Intermetallics, 2009, 17, 453-462.	3.9	76
21	Formation of a bimodal eutectic structure in Ti–Fe–Sn alloys with enhanced plasticity. Applied Physics Letters, 2008, 93, .	3.3	75
22	Structural evolution of Cu–Zr metallic glasses under tension. Acta Materialia, 2009, 57, 4133-4139.	7.9	75
23	Interfacial reaction during the fabrication of Ni60Nb40 metallic glass particles-reinforced Al based MMCs. Materials Science & Engineering A: Structural Materials: Properties, Microstructure and Processing, 2007, 444, 206-213.	5.6	74
24	Facile synthesis of CdO nanorods and exploiting its properties towards supercapacitor electrode materials and low power UV irradiation driven photocatalysis against methylene blue dye. Materials Research Bulletin, 2017, 90, 224-231.	5.2	71
25	A review on nano-/ultrafine advanced eutectic alloys. Journal of Alloys and Compounds, 2020, 827, 154226.	5.5	69
26	Facile synthesis of CuO nanowires and Cu2O nanospheres grown on rGO surface and exploiting its photocatalytic, antibacterial and supercapacitive properties. Physica B: Condensed Matter, 2019, 558, 74-81.	2.7	68
27	Fracture surface morphology of compressed bulk metallic glass-matrix-composites and bulk metallic glass. Intermetallics, 2006, 14, 982-986.	3.9	66
28	Strain distribution in Zr64.13Cu15.75Ni10.12Al10 bulk metallic glass investigated by <i>in situ</i> tensile tests under synchrotron radiation. Journal of Applied Physics, 2008, 104, .	2.5	64
29	Effect of cryorolling on the microstructure and tensile properties of bulk nano-austenitic stainless steel. Materials Science & Engineering A: Structural Materials: Properties, Microstructure and Processing, 2015, 631, 241-247.	5.6	62
30	Effect of casting conditions on microstructure and mechanical properties of high-strength Zr73.5Nb9Cu7Ni1Al9.5 in situ composites. Scripta Materialia, 2003, 49, 1189-1195.	5.2	56
31	Effect of casting conditions on dendrite-amorphous/nanocrystalline Zr–Nb–Cu–Ni–Al in situ composites. Intermetallics, 2004, 12, 1153-1158.	3.9	56
32	Work hardening ability of ductile Ti45Cu40Ni7.5Zr5Sn2.5 and Cu47.5Zr47.5Al5 bulk metallic glasses. Applied Physics Letters, 2006, 89, 071908.	3.3	56
33	Ductile Metallic Glasses in Supercooled Martensitic Alloys. Materials Transactions, 2006, 47, 2606-2609.	1.2	55
34	An assessment on the stability of the eutectic phases in high entropy alloys. Journal of Alloys and Compounds, 2019, 798, 167-173.	5.5	51
35	Deformation-induced nanostructuring in a Ti–Nb–Ta–In β alloy. Applied Physics Letters, 2006, 89, 031906.	3.3	50
36	Microstructural inhomogeneities introduced in a Zr-based bulk metallic glass upon low-temperature annealing. Materials Science & Engineering A: Structural Materials: Properties, Microstructure and Processing, 2008, 491, 124-130.	5.6	50

#	Article	IF	CITATIONS
37	Microstructure and mechanical properties of slowly cooled Cu47.5Zr47.5Al5. Journal of Materials Research, 2007, 22, 326-333.	2.6	47
38	Designing bulk metallic glass and glass matrix composites in martensitic alloys. Journal of Alloys and Compounds, 2009, 483, 97-101.	5.5	47
39	Composition Dependence on the Evolution of Nanoeutectic in CoCrFeNiNb <sub><i>x</i></sub> (0.45 â‰≇€‰ <i>x</i> â‰≇€‰0.65) High Entropy Alloys. Advanced Engineering Materials, 2018, 20, 1	7ව්ව්908.	46
40	Plasticity in bulk metallic glasses investigated via the strain distribution. Physical Review B, 2007, 76, .	3.2	45
41	Propagation of shear bands in Ti66.1Cu8Ni4.8Sn7.2Nb13.9 nanostructure-dendrite composite during deformation. Applied Physics Letters, 2005, 86, 171909.	3.3	44
42	Processing Routes, Microstructure and Mechanical Properties of Metallic Glasses and their Composites. Advanced Engineering Materials, 2007, 9, 443-453.	3.5	44
43	Martensite Formation in a Ductile Cu47.5Zr47.5Al5 Bulk Metallic Glass Composite. Advanced Engineering Materials, 2007, 9, 487-491.	3.5	44
44	Bulk ultra-fine eutectic structure in Ti–Fe–base alloys. Journal of Alloys and Compounds, 2007, 434-435, 28-31.	5.5	42
45	Strength asymmetry of ductile dendrites reinforced Zr- and Ti-based composites. Journal of Materials Research, 2006, 21, 2331-2336.	2.6	39
46	Mechanism of lamellae deformation and phase rearrangement in ultrafine β-Ti/FeTi eutectic composites. Acta Materialia, 2015, 97, 170-179.	7.9	39
47	Glass formation and mechanical properties of (Cu50Zr50)100â^'xAlx (x=0, 4, 5, 7) bulk metallic glasses. Journal of Alloys and Compounds, 2009, 483, 146-149.	5.5	38
48	Effect of Titanium on Microstructure and Mechanical Properties of Cu50Zr50â^'x Ti x (2.5Ââ‰ÅxÂâ‰Å7.5) Glass Matrix Composites. Metallurgical and Materials Transactions A: Physical Metallurgy and Materials Science, 2008, 39, 1868-1873.	2.2	36
49	Ti-base nanoeutectic-hexagonal structured (D019) dendrite composite. Scripta Materialia, 2008, 58, 631-634.	5.2	36
50	Nanostructured Composites in Multicomponent Alloy Systems. Materials Transactions, 2003, 44, 1999-2006.	1.2	34
51	Effect of twin spacing, dislocation density and crystallite size on the strength of nanostructured α-brass. Journal of Alloys and Compounds, 2015, 618, 139-145.	5.5	34
52	Strain rate dependence of plastic flow in Ce-based bulk metallic glass during nanoindentation. Journal of Materials Research, 2007, 22, 258-263.	2.6	33
53	Ti-base bulk nanostructure-dendrite composites: Microstructure and deformation. Materials Science & Engineering A: Structural Materials: Properties, Microstructure and Processing, 2007, 449-451, 24-29.	5.6	33
54	Effect of Sn on microstructure and mechanical properties of (Ti–Cu)-based bulk metallic glasses. Philosophical Magazine Letters, 2006, 86, 479-486.	1.2	32

#	Article	IF	CITATIONS
55	Propagation of shear bands in a Cu47.5Zr47.5Al5 bulk metallic glass. Journal of Materials Research, 2008, 23, 6-12.	2.6	32
56	Nano-/Ultrafine Eutectic in CoCrFeNi(Nb/Ta) High-Entropy Alloys. Transactions of the Indian Institute of Metals, 2018, 71, 2717-2723.	1.5	32
57	Structural short-range order of the β-Ti phase in bulk Ti–Fe–(Sn) nanoeutectic composites. Applied Physics Letters, 2006, 89, 261917.	3.3	31
58	Oxidation behaviour of Mo–Si–B–(Al, Ce) ultrafine-eutectic dendrite composites in the temperature range of 500–700°C. Intermetallics, 2011, 19, 1-8.	3.9	30
59	Repository on maternal child health: Health portal to improve access to information on maternal child health in India. BMC Public Health, 2013, 13, 2.	2.9	30
60	Nanostructured Composite Materials with Improved Deformation Behavior. Advanced Engineering Materials, 2005, 7, 587-596.	3.5	29
61	Formation of ductile ultrafine eutectic structure in Ti–Fe–Sn alloy. Materials Science & Engineering A: Structural Materials: Properties, Microstructure and Processing, 2007, 449-451, 737-740.	5.6	29
62	Lattice distortionâ^•disordering and local amorphization in the dendrites of a Ti66.1Cu8Ni4.8Sn7.2Nb13.9 nanostructure–dendrite composite during intersection of shear bands. Applied Physics Letters, 2005, 86, 201909.	3.3	28
63	High temperature oxidation response of Al/Ce doped Mo–Si–B composites. Intermetallics, 2017, 83, 101-109.	3.9	28
64	Microstructural investigation of a deformed Ti66.1Cu8Ni4.8Sn7.2Nb13.9 nanostructure–dendrite composite. Journal of Alloys and Compounds, 2007, 434-435, 106-109.	5.5	27
65	Deformationâ€induced microstructural heterogeneity in monolithic Zr <sub>44</sub> Ti <sub>11</sub> Cu <sub>9.8</sub> Ni <sub>10.2</sub> Be <sub>25</sub> bulk metallic glass. Physica Status Solidi - Rapid Research Letters, 2009, 3, 46-48.	2.4	27
66	Evolution of nanostructure in α-brass upon cryorolling. Materials Science & Engineering A: Structural Materials: Properties, Microstructure and Processing, 2011, 530, 675-679.	5.6	27
67	Influence of environment and grain size on magnetic properties of nanocrystalline Mn–Zn ferrite. Journal of Magnetism and Magnetic Materials, 2006, 306, 9-15.	2.3	25
68	Transient stage oxidation behavior of Mo76Si14B10 alloy at 1150°C. Corrosion Science, 2013, 68, 231-237.	6.6	25
69	High strength Ni–Zr–(Al) nanoeutectic composites with large plasticity. Intermetallics, 2015, 63, 51-58.	3.9	25
70	High strength hexagonal structured dendritic phase reinforced Zr–Ti–Ni bulk alloy with enhanced ductility. Applied Physics Letters, 2006, 88, 201920.	3.3	24
71	Effect of local chemistry, structure and length scale of heterogeneities on the mechanical properties of a Ti45Cu40Ni7.5Zr5Sn2.5 bulk metallic glass. Philosophical Magazine Letters, 2008, 88, 75-81.	1.2	23
72	Nanoscale mechanism and intrinsic structure related deformation of Ti-alloys. Materials Science & Engineering A: Structural Materials: Properties, Microstructure and Processing, 2008, 493, 71-78.	5.6	22

#	Article	IF	CITATIONS
73	Effect of Sn on microstructure and mechanical properties of Ti-Fe-(Sn) ultrafine eutectic composites. Journal of Materials Research, 2010, 25, 943-956.	2.6	22
74	Role of crystalline precipitates on the mechanical properties of (Cu0.50Zr0.50)100â^'xAlx (x=4, 5, 7) bulk metallic glasses. Journal of Alloys and Compounds, 2011, 509, S99-S104.	5.5	22
75	Origin of plasticity in ultrafine lamellar Ti-Fe-(Sn) composites. AIP Advances, 2012, 2, .	1.3	21
76	Influence of superficial CeO2 coating on high temperature oxidation behavior of Ti–6Al–4V. Journal of Alloys and Compounds, 2012, 519, 106-111.	5.5	21
77	Strengthening face centered cubic crystals by annealing induced nano-twins. Scientific Reports, 2017, 7, 17512.	3.3	20
78	Deformation behavior of a Ti66Cu8Ni4.8Sn7.2Nb14 nanostructured composite containing ductile dendrites. Journal of Alloys and Compounds, 2007, 434-435, 13-17.	5.5	19
79	Ductilization of BMGs by optimization of nanoparticle dispersion. Journal of Alloys and Compounds, 2007, 434-435, 6-9.	5.5	19
80	Evolution and interaction of twins, dislocations and stacking faults in rolled α-brass during nanostructuring at sub-zero temperature. AIP Advances, 2014, 4, .	1.3	19
81	Effect of Ce addition on the oxidation behaviour of Mo–Si–B–Al ultrafine composites at 1100 °C. Scripta Materialia, 2011, 64, 486-489.	5.2	18
82	Mechanism of microstructure evolution and spheroidization in ultrafine lamellar CoCrFeNi(NbO·5/TaO.4) eutectic high entropy alloys upon hot deformation. Materials Science & Engineering A: Structural Materials: Properties, Microstructure and Processing, 2022, 835, 142669.	5.6	18
83	Consolidation and mechanical properties of ball milled Zr50Cu50 glassy ribbons. Journal of Alloys and Compounds, 2009, 483, 227-230.	5.5	17
84	Correlation between Poisson ratio and Mohr–Coulomb coefficient in metallic glasses. Journal of Alloys and Compounds, 2009, 483, 125-131.	5.5	17
85	Mechanical response of metallic glasses: Insights from in-situ high energy X-ray diffraction. Jom, 2010, 62, 76-82.	1.9	17
86	Microscopic mechanism on the evolution of plasticity in nanolamellar Î <sup>3</sup> -Ni/Ni5Zr eutectic composites. Materials Science & Engineering A: Structural Materials: Properties, Microstructure and Processing, 2016, 666, 72-79.	5.6	15
87	Effect of Zr Addition on Microstructure, Hardness and Oxidation Behavior of Arc-Melted and Spark Plasma Sintered Multiphase Mo-Si-B Alloys. Metallurgical and Materials Transactions A: Physical Metallurgy and Materials Science, 2019, 50, 2041-2060.	2.2	15
88	A tool to predict the evolution of phase and Young's modulus in high entropy alloys using artificial neural network. Computational Materials Science, 2021, 197, 110619.	3.0	15
89	Evolution of microstructure homogeneity and mechanical properties in nano-/ultrafine eutectic CoCrFeNiNb (0.45Ââ‰ÂxÂâ‰Â0.65) high entropy alloy ingots and cast rods. Journal of Alloys and Compounds, 2022, 901, 163610.	5.5	15
90	Heterogeneous distribution of shear strains in deformed Ti66.1Cu8Ni4.8Sn7.2Nb13.9nanostructure-dendrite composite. Physica Status Solidi (A) Applications and Materials Science, 2005, 202, 2405-2412.	1.8	14

#	Article	IF	CITATIONS
91	Effect of prestraining on the deformation and fracture behavior of Zr44Ti11Cu9.8Ni10.2Be25. Intermetallics, 2010, 18, 1902-1907.	3.9	14
92	Synthesis of a robust multifunctional composite with concurrent magnetocaloric effect and enhanced energy absorption capabilities through a tailored processing route. Materials and Design, 2020, 187, 108399.	7.0	14
93	New Fe–Cr–Mo–Ga–C composites with high compressive strength and large plasticity. Acta Materialia, 2007, 55, 3513-3520.	7.9	13
94	Corrosion and pitting behaviour of ultrafine eutectic Ti–Fe–Sn alloys. Journal of Alloys and Compounds, 2010, 503, 19-24.	5.5	12
95	Improvement of oxidation resistance of arc-melted Mo 76 Si 14 B 10 by microstructure control upon minor Fe addition. Intermetallics, 2017, 88, 28-30.	3.9	12
96	Bacterial aetiology of neonatal meningitis: A study from north-east India. Indian Journal of Medical Research, 2017, 145, 138.	1.0	12
97	Microstructure and size effect in ultrafine (Ti0.705Fe0.295)100â^'xSnx (0⩽x⩽4at.%) composites. Journal Alloys and Compounds, 2014, 585, 54-62.	of 5.5	11
98	Toughening mechanisms of a Ti-based nanostructured composite containing ductile dendrites. International Journal of Materials Research, 2005, 96, 675-680.	0.8	11
99	Tailoring the microstructure and mechanical properties of Ti–Al alloy using a novel electromagnetic stirring method. Scripta Materialia, 2006, 55, 1143-1146.	5.2	10
100	Synthesis of mullite-based coatings from alumina and zircon powder mixtures by plasma spraying and laser remelting. Materials Chemistry and Physics, 2015, 154, 22-29.	4.0	10
101	Influence of Nb on the Microstructure and Fracture Toughness of (Zr0.76Fe0.24)100â^'xNbx Nano-Eutectic Composites. Materials, 2018, 11, 113.	2.9	10
102	Novel In Situ Nanostructure-Dendrite Composites in Zr-Base Multicomponent Alloy System. Materials and Manufacturing Processes, 2004, 19, 423-437.	4.7	9
103	Effect of Cold Deformation on the Machinability of a Free Cutting Steel. Materials and Manufacturing Processes, 2006, 21, 333-340.	4.7	9
104	Tuning of nanostructure by the control of twin density, dislocation density, crystallite size, and stacking fault energy in Cu 100â lx Zn x (0≤ â‰90 wt%). Materials Science & Engineering A: Structural Materials: Properties, Microstructure and Processing, 2016, 672, 203-215.	5.6	9
105	Effect of Fe addition and moist environment on the high temperature oxidation behavior of Mo76-Si14B10Fe (x = 0, 0.5, 1â€⁻at.%) composites. Intermetallics, 2019, 111, 106498.	3.9	9
106	Effect of Cold Rolling on the Evolution of Shear Bands and Nanoindentation Hardness in Zr41.2Ti13.8Cu12.5Ni10Be22.5 Bulk Metallic Glass. Nanomaterials, 2021, 11, 1670.	4.1	9
107	Effect of high pressure during the fabrication on the thermal and mechanical properties of amorphous Ni60Nb40 particle-reinforced Al-based metal matrix composites. Journal of Materials Research, 2007, 22, 1168-1173.	2.6	8
108	Impact of Microstructural Inhomogenities on the Ductility of Bulk Metallic Glasses. Materials Transactions, 2007, 48, 1806-1811.	1.2	8

#	Article	IF	CITATIONS
109	Strengthening of multicomponent glass-forming alloys by microstructure design. Journal of Non-Crystalline Solids, 2007, 353, 3742-3749.	3.1	8
110	Effect of Cu on local amorphization in bulk Ni–Ti–Zr–Si alloys during solidification. Acta Materialia, 2006, 54, 3141-3150.	7.9	7
111	Influence of annealing on the microstructure and hardness of Ti67.79Fe28.36Sn3.85 nanocomposite rods. Scripta Materialia, 2006, 55, 1087-1090.	5.2	7
112	Microstructural comparison of Zr73.5Nb9Cu7Ni1Al9.5 nanostructure-dendrite composites produced by different casting techniques. Materials Science & Engineering A: Structural Materials: Properties, Microstructure and Processing, 2007, 449-451, 747-751.	5.6	7
113	Effect of moist environment on the oxidation behavior of Mo76-Si14B10Fe (x = 0, 0.5, 1 at.%) ultrafine composites in the range of 700–800 °C. Corrosion Science, 2019, 155, 86-96.	6.6	7
114	Metallic glass formation in the Cu47Ti33Zr11Ni8Si1 alloy. Materials Science & Engineering A: Structural Materials: Properties, Microstructure and Processing, 2007, 444, 257-264.	5.6	6
115	Synthesis of crescent shaped heterocycle-fused aromatics via Garratt-Braverman cyclization and their DNA-binding studies. Tetrahedron Letters, 2017, 58, 2014-2018.	1.4	6
116	Precise estimation of glass transition and crystallization temperatures of Zr 55 Cu 30 Ni 5 Al 10 metallic glass using step-scan modulated temperature differential scanning calorimeter. Thermochimica Acta, 2018, 660, 18-22.	2.7	6
117	Synthesis, structural and magnetic properties of NiO nanospheres and rGO-NiO nanocomposites and observing magnetocaloric effect in rGO-NiO nanocomposites. Materials Science and Engineering B: Solid-State Materials for Advanced Technology, 2021, 265, 115007.	3.5	6
118	Improvement of intrinsic plasticity and strength of Zr55Cu30Ni5Al10 metallic glass by tuning the glass transition temperature. Materials Science & Engineering A: Structural Materials: Properties, Microstructure and Processing, 2019, 762, 138102.	5.6	5
119	The effect of milling time on the evolution of nanostructure, thermal stability, and magnetocaloric properties of (Ni0.50Fe0.50)70.5B17.7Si7.8Ti4. Journal of Alloys and Compounds, 2019, 772, 157-163.	5.5	5
120	Interfacial instability-driven amorphizationâ^•nanocrystallization in a bulkNi45Cu5Ti33Zr16Si1alloy during solidification. Physical Review B, 2005, 72, .	3.2	4
121	Effect of tungsten metal particle sizes on the solubility of molten alloy melt: Experimental observation of Gibbs-Thomson effect in nanocomposites. Applied Physics Letters, 2012, 101, 124103.	3.3	4
122	Effect of Oxygen Partial Pressure on the Cyclic Oxidation Behavior of Mo76Si14B10. Metallurgical and Materials Transactions A: Physical Metallurgy and Materials Science, 2013, 44, 2910-2913.	2.2	4
123	Nanoeutectic Composites: Processing, Microstructure and Properties. Transactions of the Indian Institute of Metals, 2015, 68, 1199-1205.	1.5	4
124	Correlating the lattice parameter and Curie temperature of Î <sup>3</sup> -Ni in Fe-Ni-base alloys. AIP Advances, 2019, 9, .	1.3	4
125	Accurate measurement of glass transition temperature of Cu47.5Zr47.5Al5 and Zr41.2Ti13.8Cu12.5Ni10Be22.5 using step-scan modulated differential scanning calorimeter. Journal of Alloys and Compounds, 2019, 800, 314-319.	5.5	4
126	Effect of cooling rate and composition on the microstructure and mechanical properties of (Ni0.92Zr0.08)100â^'xAlx (0 ≤ ≤ at.%) ultrafine eutectic composites. Journal of Materials Research, 2019, 34, 1704-1713.	2.6	4

#	Article	IF	CITATIONS
127	Size effect and anisotropy in cold rolled Zr-base bulk metallic glasses during nanoindentation. Journal of Non-Crystalline Solids, 2022, 593, 121767.	3.1	4
128	Influence of additional elements on the development of nanoscale heterogeneities in (TiCu)-based bulk metallic glasses with enhanced ductility. Journal of Materials Research, 2007, 22, 2223-2229.	2.6	3
129	Formation of nano-scale ω-phase in arc-melted micron-scale dendrite reinforced Zr73.5Nb9Cu7Ni1Al9.5 ultrafine composite during heat treatment. Intermetallics, 2008, 16, 538-543.	3.9	3
130	Strain rate sensitivity and deformation mechanism of nano-lamellar γ-Ni/Ni <sub>5</sub> Zr eutectic at room temperature. Journal of Materials Research, 2020, 35, 2777-2788.	2.6	3
131	Carbon nanotubes, nanochains and quantum dots synthesized through the chemical treatment of charcoal powder. Journal of Molecular Structure, 2021, 1227, 129419.	3.6	3
132	Effect of cold rolling on the pressure coefficient of glass transition temperature in bulk metallic glasses. Thermochimica Acta, 2021, 706, 179071.	2.7	3
133	Effect of cold rolling on the serrated flow behavior of Zr41.2Ti13.8Cu12.5Ni10Be22.5 bulk metallic glass during nanoindentation. Journal of Materials Research, 2022, 37, 976.	2.6	3
134	Enhanced Work Hardening of Cu-Based Bulk Metallic Glass Composites by <i>In Situ</i> Formed Nano-Scale Heterogeneities. Materials Science Forum, 2009, 633-634, 665-673.	0.3	2
135	Effect of Moist Air and Minor Zr Addition on Oxidation Behavior of Arc-Melted Multiphase Mo–Si–B Alloys in the Temperature Range of 1000°C–1300°C. Oxidation of Metals, 2020, 93, 483-513.	2.1	2
136	Strengthening ultrafine lamellar Ni-Zr-(Al) eutectic by precipitation hardening. Journal of Alloys and Compounds, 2021, 882, 160684.	5.5	2
137	Effect of testing conditions on the nanomechanical behavior of surface and inner core of as-cast Zr-base bulk metallic glassy plates. Materials Science & Engineering A: Structural Materials: Properties, Microstructure and Processing, 2022, 845, 143206.	5.6	2
138	In Situ Formed Bulk Nanostructured Ti-Base Composites. Journal of Metastable and Nanocrystalline Materials, 2005, 24-25, 31-36.	0.1	1
139	Deformation and fracture of Ti-base nanostructured composite. International Journal of Materials Research, 2008, 99, 985-990.	0.3	1
140	Stress-induced martensitic transformation in a Ti <sub>45</sub> Zr <sub>38</sub> Al <sub>17</sub> cast rod. Journal of Physics: Conference Series, 2009, 144, 012090.	0.4	1
141	A Few Aspects on the Processing and Deformation Behavior of Advanced Eutectic Alloys. Transactions of the Indian Institute of Metals, 2012, 65, 571-576.	1.5	1
142	Assessing two rapid quenching techniques for the production of Laâ€Feâ€Si magnetocaloric alloys in reduced annealing time. Material Design and Processing Communications, 2019, 1, e96.	0.9	1
143	Superior oxidation resistance of ultrafine Ni–Zr-(Al) eutectic composites in the temperature range of 500–900°C. Journal of Alloys and Compounds, 2021, 854, 155998.	5.5	1
144	Observation of superspin-glass behaviour and metamagnetic transition in spark plasma-sintered Ni50â^'xCoxMn40Sn10 (x = 3, 5, 7, and 9 at.%). Journal of Materials Research, 2022, 37, 1513-1519.	2.6	1

#	Article	IF	CITATIONS
145	Observation of a large magnetocaloric effect and suppressed transition in Ti doped Ni-Co-Mn-Sn ribbons upon annealing. Journal of Alloys and Compounds, 2022, 917, 165490.	5.5	1
146	Enhanced magnetocaloric effect in Fe-rich (NixFe1-x)70.5B17.7Si7.8Ti4 (xÂ=Â0.3 and 0.4) mechanically alloyed nanocrystalline powder. Journal of Magnetism and Magnetic Materials, 2022, 541, 168574.	2.3	0
147	How to Improve the Ductility of Nanostructured Materials. Journal of Korean Powder Metallurgy Institute, 2006, 13, 340-350.	0.3	Ο